

ABSTRACT

Traffic models are at the heart of any performance evaluation of telecommunications networks. An accurate estimation of network performance is critical for the success of broadband networks. Such networks need to guarantee an acceptable quality of service (QoS) level to the users. Therefore, traffic models need to be accurate and able to capture the statistical characteristics of the actual traffic. In this article we survey and examine traffic models that are currently used in the literature. Traditional short-range and non-traditional long-range dependent traffic models are presented. Number of parameters needed, parameter estimation, analytical tractability, and ability of traffic models to capture marginal distribution and auto-correlation structure of actual traffic are discussed.

Traffic Models in Broadband Networks

Abdelnaser Adas

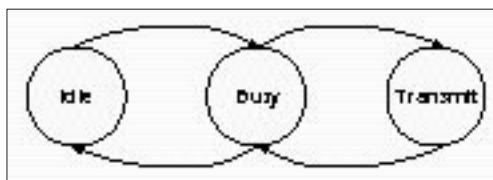
Georgia Institute of Technology

The need for telecommunication networks capable of providing diverse and emerging communication services such as data, voice, and video, motivated the standardization of broadband networks. The need for a flexible design that can accommodate future services and advances in technology led International Consultative Committee for Telephone and Telegraph (CCITT) to adopt the asynchronous transfer mode (ATM). The transfer mode is a collection of mechanisms that are used to implement switching and multiplexing in the network.

The success of ATM networks depends on the development of effective congestion control schemes. These schemes are responsible for maintaining an acceptable quality of service (QoS) level that is deliverable by the network. The congestion control schemes will decide to accept or reject new connections based on their traffic characteristics and available network resources. The congestion control schemes will police the existing connections to insure that they do not exceed their negotiated traffic characteristic parameters.

Performance modeling techniques are needed to determine which congestion control techniques should be used. Performance modeling techniques include: analytical techniques, computer simulation, and experimentation [1]. Performance models require accurate traffic models which can capture the statistical characteristics of actual traffic. If the traffic models do not accurately represent actual traffic, one may overestimate or underestimate network performance.

This article surveys traffic models in telecommunication networks. Traffic models can be stationary or nonstationary. Stationary traffic models can be classified in general into two classes: short-range and long-range dependent. Short-range dependent models include Markov processes and Regression models. These traffic models have a correlation structure that is signif-



■ Figure 1. Finite state model for voice.

icant for relatively small lags. Long-range dependent traffic models such as Fractional Autoregressive Integrated Moving Average (F-ARIMA) and Fractional Brownian motion have significant correlations even for large lags.

Traffic models are analyzed based on goodness-of-fit, number of parameters needed to describe the model, parameter estimation, and analytical

tractability. To evaluate goodness-of-fit, one needs to define metrics that determine how "close" the model is to the actual data [2]. These metrics have to be directly related to the performance measures that are needed to be predicted from the model. The goodness-of-fit used in this article is based on the ability of the model to capture marginal distributions, auto-correlation structure, and ultimately predict delays and cell loss probabilities.

This article is organized as follows: The second and third sections cover traditional traffic models, Markov, and Regression models. The fourth section discusses nontraditional traffic models. It briefly reviews long-range dependence and discusses three different long-range dependent traffic models, fractional Brownian motion, F-ARIMA, and aggregation of high-variability ON-OFF sources. Finally, the fifth section concludes the article.

MARKOV AND EMBEDDED MARKOV MODELS

In many situations, the activities of a source can be modeled by a finite number of states. Figure 1 shows a widely used finite state model in voice telephony. In this model, a voice source is either idle or busy. When it is busy, it will only transmit packets during speech activity. In general, increasing the number of states results in a more accurate model at the expense of increased computational complexity.

For a given state space $S = \{s_1, s_2, \dots, s_M\}$, let X_n be a random variable which defines the state at time n . The set of random variables $\{X_n\}$ will form a discrete Markov chain, if the probability of the next value $X_{n+1} = s_j$ depends only on the current state. This is known as Markov property [3]. If state transitions occur at integer values $(0, 1, \dots, n, \dots)$, the Markov chain is discrete time. Otherwise, the Markov chain will be continuous time.

Markov property implies that the future depends on the

This research was supported in part by the National Science Foundation under grant NCR-9396299. This article is based on Georgia Tech technical report GIT-CC-96-01.

current state and not on previous states nor on the time already spent in the current state. This restricts the random variable, which describes the time spent in a state to a geometric distribution in the discrete case and to an exponential distribution in the continuous case [3].

A semi-Markov process is obtained by allowing the time between state transitions to follow an arbitrary probability distribution. If the time distribution between transitions is ignored, the sequence of states visited by the semi-Markov process will be a discrete time Markov chain, and is referred to as an embedded Markov chain.

In a simple Markov traffic model, each state transition represents a new arrival. Therefore, inter-arrival times are exponentially distributed (for continuous time case), and their rates depend on the state from which the transition occur [1]. The rest of this section discusses various Markov and embedded Markov models that have been used to model network traffic.

ON-OFF AND IPP MODELS

The ON-OFF source model shown in Fig. 2a is the most popular source model for voice [4, 5]. In this model, packets are only generated during talk spurts (ON state) with fixed inter-arrival time. The time spent in ON and OFF states is exponentially distributed with mean α^{-1} and β^{-1} , respectively.

The interrupted Poisson process (IPP) shown in Fig. 2b is also a two-state process. Arrivals only occur in the active state according to a Poisson distribution with rate λ . Hence, IPP and ON-OFF models differ in interarrival time during the active (ON) state.

ALTERNATING STATE RENEWAL PROCESS

The alternating state renewal process is a two state process [6], s_1 and s_2 , with no self transition. Therefore, the embedded Markov chain is alternating between s_1 and s_2 . The traffic amplitude is 0 while in state s_1 and 1 while in state s_2 . Let the mean sojourn time in s_1 and in s_2 to be d_1 and d_2 , respectively. Then, the steady state probabilities for being in state s_1 is $P_{s_1} = d_1/(d_1 + d_2)$, and for s_2 is $P_{s_2} = d_2/(d_1 + d_2)$.

The superposition of identical independent alternating state renewal processes has a binomial distribution [6].

MARKOV MODULATED POISSON PROCESS

A Markov modulated process, also called doubly stochastic process, uses an auxiliary Markov process in which the current state of the Markov process controls (modulate) the probability distribution of the traffic.

Markov modulated Poisson process (MMPP) uses Poisson process as the modulated mechanism as shown in Fig. 3. In this model, while in state s_k , the arrivals occur according to a Poisson process with rate λ_k . The introduction of MMPP process allows the modeling of time-varying sources while keeping the analytical solution of related queuing performance tractable.

The MMPP parameters can be estimated easily from the empirical data as follows: quantize the arrival rate into finite number of rates which corresponds to the number of states. Each rate corresponds to a state in the Markov chain. The transition rate from state i to state j , denoted by q_{ij} , is estimated by quantizing the empirical data and by calculating the fraction of times that the state (rate) i switched to state (rate) j . Note that an MMPP process with $M + 1$ states can be obtained by the superposition of M identical independent IPP sources.

MMPP can model a mixture of voice and data traffic. In this case, the arrivals of voice packets while in state k is assumed to be Poisson with rate λ_k . Data packets are also Poisson with rate λ_d . The resulting rate of state s_k will be $\lambda_d + \lambda_k$. The performance measures such as queuing distribution and the moments of the delay distribution are obtained using MMPP/G/1 queue analysis [4].

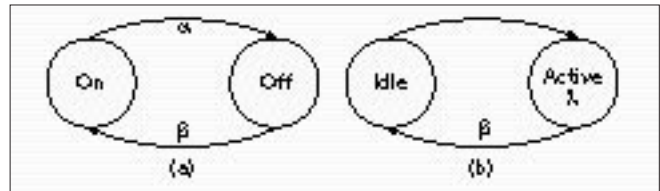


Figure 2. a) ON-OFF model and b) IPP model.

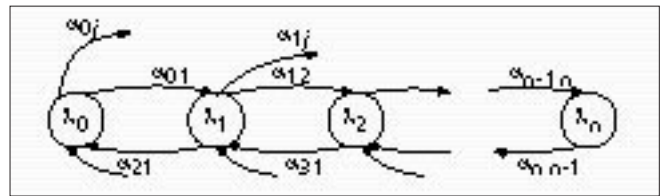


Figure 3. MMPP process.

MARKOV MODULATED FLUID MODELS

Fluid models characterize the traffic as a continuous stream with a parameterized flow rate (such as bits/sec). These models are appropriate in the case where individual units of traffic (packets or cells) have little impact on the performance of the network.

Fluid models are conceptually simple and their simulation has an important advantage over other models. Consider for example, an event simulation for an ATM multiplexer. All models that distinguish between cells and consider the arrival of each cell as a separate event, consume vast amount of memory and CPU resources. In contrast, fluid models characterize the incoming cells by a flow rate. An event is only triggered when the flow rate changes. Since flow rate changes happen much less frequently than cell arrivals, considerable savings in computing and memory resources are achieved [1].

A fluid model that is typically used to model traffic is the Markov modulated fluid model. In this model, the current state of the underlying Markov chain determines the flow (traffic) rate. While in state s_k , traffic arrives at a constant rate λ_k . This model is a Markov modulated constant rate model and is used in [7, 8] to model VBR video sources.

In [7], the continuous bit rate is quantized into a finite set of discrete levels and sampled at random Poisson points (i.e., inter-sample time is exponentially distributed), as shown in Fig. 4. The number of states in the Markov chain is equal to the number of quantized levels. Since Markov processes have exponentially decaying auto-covariance function, the auto-covariance of the empirical data is approximated by $C(\tau) = Ce^{-a\tau}$.

There are many Markov chains that satisfy the above auto-covariance function and the average of the empirical data. The birth-death Markov chain shown in Fig. 5 is used for its simplicity in [8]. In this model, the bit rate while in state i is constant and is given by iA , where A is the quantization step size. The transition rates are chosen such that lower bit-rate-states tend to jump to higher-bit-rate states and vice-versa. This model captured approximately the first 10 lags of the auto-correlation function of the empirical data. This is due to a faster decay in the auto-correlation function of the model than the auto-correlation function of the actual data. Moreover, jumps are only allowed to neighboring states in birth-death Markov chain, so the model lacks the ability to capture abrupt changes in the arrival rate between frames.

In order to capture scene changes in the above model, [7] extended the model by allowing the rate to be integer multiples of two basic levels: high level A_h , and low level A_l . It uses a two-dimensional Markov chain in which the state is defined by two indices i and j , where $0 \leq i \leq M$ and $0 \leq j \leq N$. While in state (i, j) , the flow rate is $iA_l + jA_h$. Fig. 6 illustrates the case when $M = 1$ and $N = N_p$.

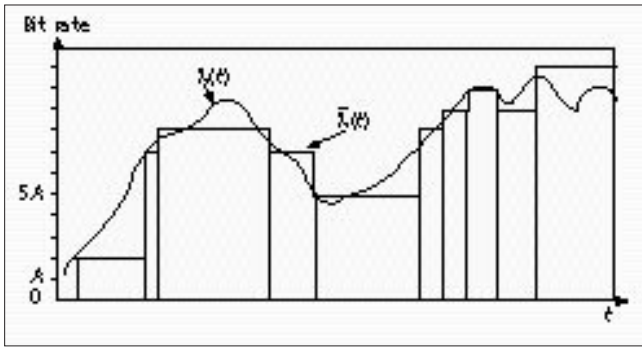


Figure 4. Approximation of continuous source rate $\lambda(t)$ using Poisson sampling and quantization by modulated fluid flow $\bar{\lambda}(t)$.

The queuing performance of this model is still analytically tractable and it has been considered in [8]. The model has many parameters, and exponentially decaying auto-correlation function. The complexity of analytical solution increases by adding more activity levels.

REGRESSION MODELS

Regression models define explicitly the next random variable in the sequence by previous ones within a specified time window and a moving average of a white noise. In this section several regression models are presented.

AUTOREGRESSIVE MODELS

The Autoregressive model of order p , denoted as AR(p), has the following form:

$$X_t = \phi_1 X_{t-1} + \phi_2 X_{t-2} + \dots + \phi_p X_{t-p} + \varepsilon_t \quad (1)$$

where ε_t is white noise, ϕ_j 's are real numbers, and X_t 's are prescribed correlated random variables. If ε_t is a white Gaussian noise with variance $\sigma_{\varepsilon_t}^2$, then X_t 's will be normally distributed random variables. Let us define a lag operator B as $X_{t-1} = BX_t$, and let $\phi(B)$ be a polynomial in the operator B , defined as follows: $\phi(B) = (1 - \phi_1 B - \dots - \phi_p B^p)$. Then, the AR(p) process can be represented as:

$$\phi(B)X_t = \varepsilon_t \quad (2)$$

The process $\{X_t\}$ is stationary if the roots of $\phi(B)$ lie outside the unit circle [10]. The auto-correlation ρ_k can be computed by multiplying Eq. (1) with X_{t-k} , taking the expectation, and dividing by the variance γ_0 :

$$\rho_k = \phi_1 \rho_{k-1} + \phi_2 \rho_{k-2} + \dots + \phi_p \rho_{k-p}; \text{ for } k > 0. \quad (3)$$

Thus, the general solution is

$$\rho_k = A_1 G_1^k + A_2 G_2^k + \dots + A_p G_p^k, \quad (4)$$

where G_i^{-1} 's are the roots of $\phi(B)$. Therefore, the auto-correlation function of AR(p) process will consist, in general, of damped exponentials, and/or damped sine waves depending on whether the roots are real or imaginary.

Since successive video frames do not vary much visually, AR models have been used to model the output bit rate of VBR encoder [7, 11]. In [7], a video source is approximated by a continuous fluid flow model. In the model, the output bit rate within a frame period is constant and changes from frame to frame according to the following AR(1) model:

$$\lambda[n] = \phi \lambda[n-1] + b \varepsilon[n], \quad (5)$$

where $\lambda[n]$ is the bit rate during frame n and $\varepsilon[n]$ is a Gaussian white noise. $\varepsilon[n]$ is chosen such that the probability of $\lambda[n]$ being negative is very small. Since the number of bits in frame n cannot be negative, the value of $\lambda[n]$ in Eq. 5 is set to

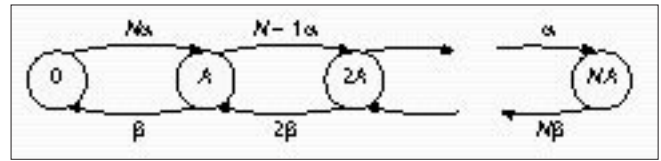


Figure 5. State transition diagram for birth-death Markov chain.

zero, whenever $\lambda[n]$ is negative. This model, cannot capture abrupt changes in the frame bit rates that occur due to scene changes or visual discontinuities. Therefore, one may model the bit rate of frames within the scene as an AR process and model the scene changes by an underlying Markov chain.

In [11], VBR video traffic is modeled as $X_n = Y_n + Z_n + V_n C_n$. Y_n and Z_n are two independent AR(1) processes. These two AR processes are used to get a better fit of the auto-correlation function of the empirical data than using only one AR(1) process. The last term, $V_n C_n$, is the product of a 3-state Markov chain and an independent normal random variable. It is designed to capture sample path spikes due to video scene changes. This may work for encoding techniques in which only the difference between the frames and a reference frame is encoded and transmitted. Reference frames are transmitted when the difference is greater than a certain threshold. They, in general, indicate a scene change. Reference frames have higher bit rates than the other surrounding frames and they cause the spikes in the sample path of the bit rate of the video stream. In MPEG, a scene change detection is not trivial due to periodically transmitting a reference frame (I frame).

Although it is easy to estimate the AR model parameters and to generate the sequence recursively, the exponential decay of the auto-correlation function makes the model unable to capture auto-correlation functions that decay at a slower rate than the exponential. AR is approximated in [7] by a Markov modulated fluid model, in order to obtain analytical queuing performance results. AR processes with Gaussian distribution cannot capture VBR video traffic probability distribution. Since VBR video traffic distribution exhibits a heavier tail behavior than the Gaussian.

DISCRETE AUTOREGRESSIVE MODELS

A Discrete Autoregressive model of order p , denoted as DAR(p), generates a stationary sequence of discrete random variables with an arbitrary probability distribution and with an auto-correlation structure similar to that of an AR(p).

DAR(1) is a special case of DAR(p) process and it is defined as follows: let $\{V_n\}$ and $\{Y_n\}$ be two sequences of independent random variables. The random variable V_n can take two values 0 and 1, with probabilities, $1 - \rho$ and ρ , respectively. The random variable Y_n has a discrete state space S and $P\{Y_n = i\} = \pi(i)$. The sequence of random variables $\{X_n\}$ which is formed according to the linear model:

$$X_n = V_n X_{n-1} + (1 - V_n) Y_n$$

is a DAR(1) process. DAR(1) process is a Markov chain with discrete state space S and a transition matrix:

$$\mathbf{P} = \rho \mathbf{I} + (1 - \rho) \mathbf{Q},$$

where \mathbf{I} is the identity matrix and \mathbf{Q} is a matrix with for $Q_{ij} = \pi(j)$ for $i, j \in S$. DAR(1) has a correlation structure of a first-order autoregressive process with $\rho_k = \rho^k$ and has the probability distribution function of π . In [12-14] the number of cells per frame of teleconferencing VBR video is modeled by DAR(1) with negative binomial distribution. The rows of the \mathbf{Q} matrix consist of the negative-binomial probabilities $(f_0, f_1, \dots, f_K, F_K^c)$, where $F_K^c = \sum_{k > K} f_k$, and K is the peak rate. Therefore, only mean, variance, peak rate, and the first auto-correlation coefficient are needed to be estimated from the data.

DAR(1) has far less number of parameters than the general Markov chains. The parameter estimation is simple. The distribution of the resulting process is arbitrary. Moreover, the analytical queuing performance is tractable. On the other hand, the auto-correlation function decays exponentially and hence it cannot be used to model traffic with a slower auto-correlation decay.

AUTOREGRESSIVE MOVING AVERAGE MODELS

An Autoregressive Moving Average model of order (p, q) , denoted as ARMA (p, q) , has the form

$$X_t = \phi_1 X_{t-1} + \phi_2 X_{t-2} + \dots + \phi_p X_{t-p} + \varepsilon_t - \theta_1 \varepsilon_{t-1} - \theta_2 \varepsilon_{t-2} - \dots - \theta_q \varepsilon_{t-q} \quad (6)$$

which can be equivalently represented as:

$$\phi(B)X_t = \theta(B)\varepsilon_t \quad (7)$$

where B and $\phi(B)$ are as defined previously, and $\phi(B) = (1 - \theta_1 B - \dots - \theta_q B^q)$.

This is equivalent to filtering a white noise process ε_t by a causal linear shift time invariant filter having a rational system function with p poles and q zeros [15]; that is,

$$H(z) = \frac{B_q(z)}{A_p(z)} = \frac{1 - \sum_{k=0}^q \theta_k z^{-k}}{1 - \sum_{k=1}^p \phi_k z^{-k}} \quad (8)$$

The auto-covariance γ_k of the ARMA (p, q) process can be obtained by multiplying Eq. 6 with X_{t-k} , taking the expectation, and finding the cross-correlation between ε_t and X_t

$$\gamma_k = \phi_1 \gamma_{k-1} + \dots + \phi_p \gamma_{k-p} - \sigma_\varepsilon^2 (\theta_k h_0 + \theta_{k+1} h_1 + \dots + \theta_q h_{q-k}) \quad (9)$$

where h_t is the impulse response of the ARMA (p, q) filter $H(z)$.

Note that $\theta_k = 0$ for $k > q$, therefore, the auto-correlation of the process for $k > q$

$$\rho_k = \phi_1 \rho_{k-1} + \phi_2 \rho_{k-2} + \dots + \phi_p \rho_{k-p}; \text{ for } k > q, \quad (10)$$

which is the same difference equation as Eq. 3, therefore, the auto-correlation of the ARMA (p, q) decays exponentially.

An ARMA model is used in [16] to model VBR traffic. The duration of a video frame is equally divided into m time intervals. The number of cells in the n^{th} time interval is modeled by the following ARMA process:

$$X_n = \phi X_{n-m} + \sum_{k=0}^{m-1} \theta_k \varepsilon_{n-k}$$

Since video data will correlate at each frame due to temporal correlation, the auto-correlation function has peaks at all lags which are integer multiples of m . In the above model, the AR part is used to model the recorelation effect and the θ_k 's are used to fit the correlation at other lags.

The parameter estimation of ARMA models are more involved than that of AR models, the estimation of the θ_k 's require solving a set of non-linear equations or using spectral factorization techniques [15]. The analytical solutions are also difficult to obtain.

AUTOREGRESSIVE INTEGRATED MOVING AVERAGE MODELS

The Autoregressive Integrated Moving Average model of order (p, d, q) , denoted as ARIMA (p, d, q) , is an extension to the ARMA (p, q) . It is obtained by allowing the polynomial $\phi(B)$ to have d roots equal to unity. The rest of the roots lie outside the unit circle. The ARIMA (p, d, q) has the form:

$$\phi(B)\nabla^d X_t = \theta(B)\varepsilon_t \quad (11)$$

where ∇ is a difference operator, defined as $(X_t - X_{t-1}) = \nabla X_t$,

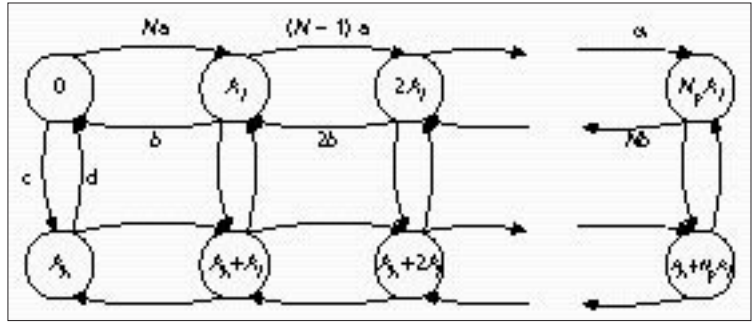


Figure 6. Fluid flow model for two level of activity VBR sources.

and $\phi(B)$ is a polynomial in B . Notice that $\nabla X_t = (1 - B)X_t$. The ARIMA (p, d, q) is used to model homogeneous nonstationary time series. For example, a time series that exhibits nonstationarity in level, or in level and slope, can be modeled by using ARIMA $(p, 1, q)$ and ARIMA $(p, 2, q)$, respectively [17].

TES MODELS

Transform-expand-sample (TES) models are non-linear regression models with modulo-1 arithmetic. They aim to capture both auto-correlation and marginal distribution of empirical data.

TES models consist of two major TES processes [1, 18, 19]: TES^+ and TES^- . TES^+ produces a sequence which has positive correlation at lag 1, while TES^- produces a negative correlation at lag 1.

Before describing TES^+ or TES^- , we need to introduce a few definitions and notations. The modulo-1 of a real number x , denoted as $\langle x \rangle$, is defined as $\langle x \rangle = x - \lfloor x \rfloor$, where $\lfloor x \rfloor$ is the maximum integer less than x . Therefore, $\langle x \rangle$ is always non-negative. If the interval $[0,1)$ is viewed as a circle that is obtained by joining the points 0 and 1, one can define a circular interval $C[a, b)$, where a and $b \in [0,1)$, as all the points on the circular unit interval going clockwise from point a to point b . Therefore:

$$C[a, b) = \begin{cases} [a, b), & \text{if } a \leq b \\ [0,1) - [b, a), & \text{if } a > b \end{cases}$$

TES^+ and TES^- — $TES^+(L, R)$ is introduced in [19] and is characterized by two parameters, L and R . The sequence $\{U_n^+\}$ is generated recursively as follows: initialize $U_0^+ = U_0$, where U_0 is uniform in the interval $(0,1)$. Then U_n^+ is a uniformly sampled random variable on the circular interval $C_{U_{n-1}^+} = [\langle U_{n-1}^+ - L \rangle, \langle U_{n-1}^+ + R \rangle)$.

In the $TES^-(L, R)$, the sequence is generated as in TES^+ with U_n^- is uniform random variable over the circular interval:

$$C_{U_{n-1}^-}[a, b) = \begin{cases} [\langle 1 - U_{n-1}^- - L \rangle, \langle 1 - U_{n-1}^- + R \rangle), & n \text{ even} \\ [\langle 1 - U_{n-1}^- - R \rangle, \langle 1 - U_{n-1}^- + L \rangle), & n \text{ odd} \end{cases}$$

TES^+ and TES^- can also be characterized by $\alpha = L + R$, and $\phi = (R - L)/\alpha$. Note that α represents the length of the circular interval. The sample path realizations generated by simulation using TES^+ and TES^- have shown discontinuity due to the crossing of the 0 point on the unit circular interval from both directions. For example, crossing clockwise will result in a jump from small values to large values. It was shown in [19] that a continuous sample path realization can be obtained by using a simple piece wise transformation T_ξ called stitching, where:

$$T_\xi = \begin{cases} \frac{x}{\xi}, & x \in [0, \xi) \\ \frac{1-x}{1-\xi}, & x \in [\xi, 1) \end{cases}$$

Autocorrelation of TES^+ and TES^- — The lag-1 auto-correlation for TES processes is derived in [19] and is given by:

$$\rho_1^+(\alpha, \phi) = 1 - \frac{3+3\phi^2}{2}\alpha + \frac{1+3\phi^2}{2}\alpha^2. \quad (12)$$

$$\rho_1^-(\alpha, \phi) = -1 + \frac{3+3\phi^2}{2}\alpha - \frac{1+3\phi^2}{2}\alpha^2. \quad (13)$$

The auto-correlation for higher-order lags is simulated in [19] and its computation is presented in [18]. The value of α affects the magnitude of the correlation, while the value of ϕ affects the oscillating behavior of the auto-correlation. The larger the α , the smaller the magnitude. If $\phi = 0$, there will be no oscillation. For $\phi \neq 0$, the larger the ϕ , the faster the oscillation.

In [18], the definitions in [19] are generalized. The recursive construction of the underlying TES processes is defined as follows:

$$U_n^+ = \begin{cases} U_0, & n = 0 \\ \langle U_{n-1}^+ + V_n \rangle, & n > 0 \end{cases}$$

$$U_n^- = \begin{cases} U_n^+, & n \text{ even} \\ 1 - U_n^+, & n \text{ odd} \end{cases}$$

Here, $\{V_n\}$ is a sequence of independent identically distributed random variables independent from U_0 . The resulting sequences $\{U_n^+\}$ and $\{U_n^-\}$ are uniformly distributed in $[0, 1)$ no matter what the density function of V_n , denoted as f_V [1, 18]. The choice of f_V will result in a different correlation structure of the resulting process.

The targeted sequences $\{X_n^+\}$ and $\{X_n^-\}$ are then obtained by using the inversions $\{X_n^+\} = D(U_n^+)$ and $\{X_n^-\} = D(U_n^-)$, where $D = F^{-1}$ and F is the marginal distribution of the desired sequence (the empirical data). The fitting of the auto-correlation is done by a heuristic search for a pair (ξ, f_i) [1]. A combination of TES processes can also be used to better fit the auto-correlation. The empirical distribution is matched using the distribution inversion methods. The auto-correlation function of TES processes decays exponentially.

LONG-RANGE DEPENDENT TRAFFIC MODELS

Stationary traffic models presented in the second and third sections have a correlation structure that is characterized by an exponential decay. A recent analysis of traffic measurements of Ethernet LAN traffic [20] and NSFNET [21], has suggested that the auto-correlation decays to zero at a slower rate than exponential. This slow decay in correlation has been observed before in other statistical applications, e.g., hydrology [22]. Mathematical models have been developed to capture this behavior [23, 24].

BACKGROUND ON LONG-RANGE DEPENDENCE

Let $\{X_t\}$, $t = 0, 1, 2, \dots$ be a wide-sense stationary stochastic process, i.e., a process with a stationary mean $\mu = E[X_t]$, a stationary and finite variance $v = E[(X_t - \mu)^2]$, and a stationary auto-covariance function $\gamma_k = E[(X_t - \mu)(X_{t+k} - \mu)]$, that depends only on k and not on t . Observe that $v = \gamma_0$. Let the auto-correlation of $\{X_t\}$ at lag k be denoted as ρ_k , where by definition, $\rho_k = \gamma_k/\gamma_0$.

For each m , let $\{X_j^{(m)}\}$ denote a new time series obtained by averaging the original series $\{X_t\}$ over non-overlapping blocks of size m , i.e.,

$$X_j^{(m)} = \frac{1}{m}(X_{jm-m+1} + \dots + X_{jm}). \quad (14)$$

Observe that $X_j^{(m)}$ is the sample mean of $S_{jm-m+1} + \dots + X_{jm}$. Let v_m denote the variance of $\{X_j^{(m)}\}$ and it is given by [17, 25]:

$$v_m = E\left[\frac{1}{m}(X_{jm-m+1} + \dots + X_{jm})\right]^2 \quad (15)$$

$$- \left[E \frac{1}{m}(X_{jm-m+1} + \dots + X_{jm}) \right]^2,$$

$$= \frac{v}{m} + \frac{2}{m^2} \sum_{k=1}^m (m-k)\gamma_k, \quad (16)$$

$$= v \left[1 + 2 \sum_{k=1}^m \left(1 - \frac{k}{m}\right) \rho_k \right] m^{-1} \quad (17)$$

Hence, if the process is white noise, $X_{jm-m+1}, \dots, X_{jm}$ will be mutually uncorrelated, i.e., $\rho_k = 0$ for $k > 0$, and $v_m = vm^{-1}$.

For large m Eq. 17 can be approximated by:

$$v_m = v \left[2 \sum_{k=1}^m \rho_k \right] m^{-1}. \quad (18)$$

Consider the case in which $\rho_k \neq 0$ and $\sum_{k=-\infty}^{\infty} \rho_k < \infty$. The variance of the sample mean will asymptotically decay to zero proportional to m^{-1} , i.e.,

$$v_m \approx v c_p m^{-1}, \quad (19)$$

where c_p is constant. Time series models such as ARMA and Markov processes have a sample mean variance that decays asymptotically according to Eq. 19.

Recently, several traffic measurements (see, e.g., [20, 21, 26]) have shown that the sample mean variance, v_m , decays at a slower rate than m^{-1} . One simple approach to model this decay explicitly, is to have v_m decay proportional to $m^{-\alpha}$ for some $\alpha \in (0, 1)$. This requires that $\sum_{k=1}^m \rho_k$ to be proportional to $m^{1-\alpha}$, that is,

$$\sum_{k=1}^m \rho_k \approx C m^{1-\alpha}.$$

Since $\alpha < 1$, this implies

$$\sum_{k=-\infty}^{\infty} \rho_k \rightarrow \infty.$$

Thus, the auto-correlation decays slowly in a way that it is not summable. An example of such an auto-correlation function is

$$\rho_k \approx C \rho |k|^{-\alpha}, \text{ for large } k. \quad (21)$$

Short-Range and Long-Range Dependence — The process $\{X_t\}$ is said to have a short-range dependence, if $\sum_k \rho_k < \infty$. Equivalently, v_m decays asymptotically proportional to m^{-1} , the power spectral density has a finite value at zero, and the averaged process $\{X_t^{(m)}\}$, tends to second order pure noise as $m \rightarrow \infty$. Processes that have auto-correlation functions that decay exponentially, are short-range dependent processes. a) shows an example of an auto-correlation of a short-range dependent process.

The process $\{X_t\}$ is said to have long-range dependence, if $\sum_k \rho_k \rightarrow \infty$ [17]. Since the power spectral density function is defined as $\sum_k \rho_k e^{-j\omega k}$. Therefore, the power spectral density function is singular near zero, that is, it increases without a limit as the frequency tends to zero. The variance of the sample mean v_m decays at a slower rate than m^{-1} . For example, processes in which $\rho_k \sim Ck^{-\alpha}$ (for large k), where $\alpha \in (0, 1)$ are long-range dependent and their v_m decay proportional to $m^{-\alpha}$. Figure 7b shows an auto-correlation function of a long-range dependent process.

It is important to note that the definition of long-memory dependence is an asymptotic definition [25]. It only describes the behavior of the auto-correlation at large lags. It does not specify the auto-correlation for any fixed finite lag.

Self-Similarity — The process $\{X_t\}$ is said to be exactly (second-order) self-similar if $\rho_k^{(m)}$ for all m and k i.e., the correla-

tion structure is preserved across different time scales. The process $\{X_t\}$ is said to be asymptotically self similar, if $\rho_k^{(m)} \rightarrow \rho_k$ for m and k large [27].

Stochastic self-similar processes retain the same statistics over a range of scales, and they satisfy the following relation:

$$\{X_{at}\} \stackrel{D}{=} a^H \{X_t\},$$

where $\stackrel{D}{=}$ denotes equality in distribution and H is called the Hurst parameter [28]. Therefore, the sample paths appear to be qualitatively the same, irrespective of the time scale. This does not mean that the same picture repeats itself exactly as in deterministic self-similarity. It is the general impression "odds" that remains the same [25].

If $\{X_t\}$ has stationary increments, then the increment process $Y_t = X_t - X_{t-1}$ has an auto-correlation of the form:

$$\rho_k \rightarrow H(2H - 1)k^{2H-2}, \text{ as } k \rightarrow \infty \quad (22)$$

This can be verified by using the self-similarity definition $\{X_t\} \stackrel{D}{=} t^H \{X_1\}$, defining $\sigma^2 = E(X_t - X_{t-1})^2 = E(X_1^2)$ the variance of the increment process $\{Y_t\}$, and finding the covariance of the increment process $\{Y_t\}$ [25]. By comparing Eq. 22 to Eq. 21, then $H = 1 - \alpha/2$. Note that for $H \in (0, 1)$ and $H \neq 1/2$, $\sum_k \rho_k \rightarrow \infty$. Fractional Gaussian noise is an example of an exactly self-similar process and Fractional ARIMA is an example of an asymptotically self-similar process.

FRACTIONAL ARIMA

The fractional Autoregressive Integrated Moving Average process, F-ARIMA(p, d, q) with $0 < d < 1/2$, is an example of a stationary process with long-range dependence. It is an extension to ARIMA(p, d, q) and defined as:

$$\phi(B)\nabla^d X_t = \theta(B)\varepsilon_t \quad (23)$$

where d can take values between 0 and 1/2. The operator $\nabla^d = (1 - B)^d$ can be expressed using the binomial expansion [25]

$$(1 - B)^d = \sum_{k=0}^{\infty} \binom{d}{k} (-1)^k B^k, \quad (24)$$

$$\binom{d}{k} = \frac{d!}{k!(d-k)!} = \frac{\Gamma(d+1)}{\Gamma(k+1)\Gamma(d-k+1)} \quad (25)$$

where $\Gamma(x)$ denotes the gamma function. Note that for all positive integers, only the first $d + 1$ terms are non-zero in Eq. 25. That is because the gamma function has poles for negative integers and hence the binomial coefficients are zero if $k > d$ and d is an integer. The representation in Eq. 25 for ∇^d is equivalent to an infinite order autoregressive process (all pole filter with an infinite order). F-ARIMA(0, d , 0) process with $0 < d < 1/2$, is stationary and long-range dependent, with an auto-correlation function [29]

$$\rho_k = \frac{\Gamma(1-d)\Gamma(k+d)}{\Gamma(d)\Gamma(k+1-d)} \sim \frac{\Gamma(1-d)}{\Gamma(d)} k^{2d-1} \text{ as } k \rightarrow \infty. \quad (26)$$

Observe that for $0 < d < 1/2$, the hyperbolic decay will produce persistence. By comparing Eq. 26 to Eq. 21, $d = (1 - \alpha)/2 = H - 0.5$. F-ARIMA processes can model short-range and long-range dependence. If Gaussian white noise is used, then the F-ARIMA has a Gaussian distribution. This limits the ability of F-ARIMA to model processes which have an approximately Gaussian distributions. The Gaussian white noise is used because the sum of two Gaussian random variables is a Gaussian random variable. This is also true for a class of random variables called Stable random variables that include Gaussian random variables [28].

One way to estimate d is the variance-time-plot method. In this method, the $Var(\{X^{(m)}\}) = v_m$ is plotted versus the aggregation level m (on log-log scale). The asymptotic slope $-\alpha$ is then, esti-

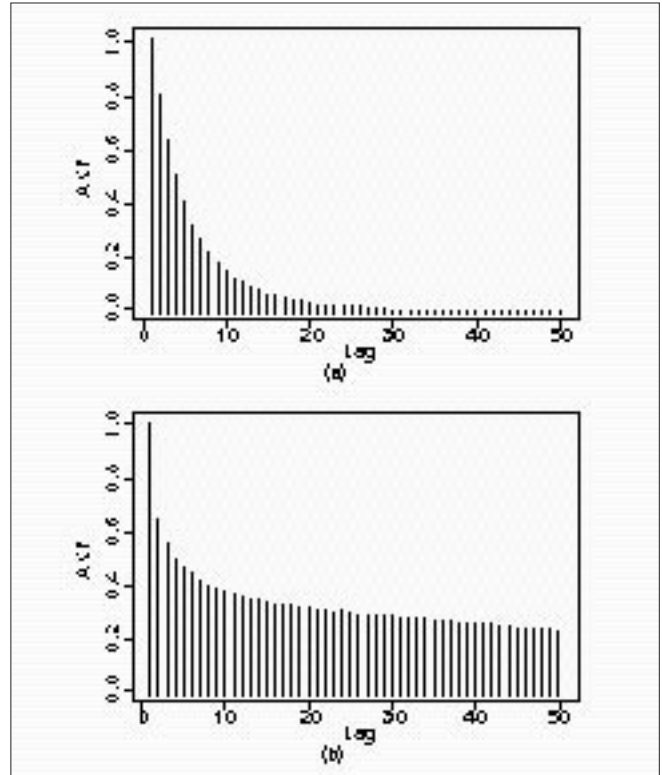


Figure 7. Examples of auto-correlation structures of a) short-range dependent process, b) long-range dependent process.

mated and the value of $d = (1 - \alpha)/2$ is obtained. F-ARIMA was used to model VBR video traffic [26, 30] and the queuing performance of F-ARIMA(1, d , 0) was analyzed through simulation for a first come first served (FCFS) queue in [31].

FRACTIONAL BROWNIAN MOTION

Brownian motion is a stochastic process, denoted, $\{B_t\}$, for $t \geq 0$. It is characterized by the following properties [32]:

- The increments $B_{t_1} - B_{t_0}$ are normally distributed with mean 0 and variance $\sigma^2 t$.
- The increments in non-overlapping time intervals $[t_1, t_2]$ and $[t_3, t_4]$, i.e., $B_{t_2} - B_{t_1}$ and $B_{t_4} - B_{t_3}$ are independent random variables.
- $B_0 = 0$ and B_t is continuous at $t = 0$.

The fractional Brownian motion $\{fB_t\}$ is a Gaussian self-similar process with self-similarity parameter $H \in [0.5, 1)$ [33]. Fractional Brownian motion differs from the Brownian motion by having increments with variance $\sigma^2 t^{2H}$. Define $\sigma^2 = E\{(fB_t - fB_{t-1})^2\} = E\{(fB_1 - fB_0)^2\} = E\{fB_1^2\}$ the variance of the increment process (Note that $fB_0 = 0$). Then:

$$E\{(fB_{t_2} - fB_{t_1})^2\} = E\{(fB_{t_2-t_1} - fB_0)^2\} = \sigma^2 (t_2 - t_1)^{2H}.$$

Also:

$$E\{(fB_{t_2} - fB_{t_1})^2\} = E\{(fB_{t_2}^2) + E\{(fB_{t_1}^2) - 2E\{fB_{t_2} fB_{t_1}\}\} = \sigma^2 t_2^{2H} + \sigma^2 t_1^{2H} - 2\gamma(fB_{t_1}, fB_{t_2}),$$

$$\gamma(fB_{t_1}, fB_{t_2}) = 1/2 \sigma^2 (t_2^{2H} - (t_2 - t_1)^{2H} + t_1^{2H}).$$

Hence, the covariance of increments in two nonoverlapping intervals is given by:

$$\begin{aligned} \gamma(fB_{t_4} - fB_{t_3}, fB_{t_2} - fB_{t_1}) &= \\ \gamma(fB_{t_4}, fB_{t_2}) - \gamma(fB_{t_4}, fB_{t_1}) - \gamma(fB_{t_3}, fB_{t_2}) &+ \gamma(fB_{t_3}, fB_{t_1}), \\ &= \sigma^2/2 (t_4 - t_1)^{2H} - (t_3 - t_1)^{2H} \\ &+ (t_3 - t_2)^{2H} - (t_4 - t_2)^{2H}. \end{aligned} \quad (27)$$

The fractional Brownian motion $\{fB_t\}$ can be deduced from Brownian motion $\{B_t\}$ [24, 25] by forming the integral:

$$fB_t = \int_0^t (t-u)^{H-0.5} dB(u).$$

As Eq. 28 shows, the interdependence between the increments of the fractional Brownian motion can be said to be infinite.

In the discrete case [25], the auto-correlation of the increment sequence is obtained by replacing $t_1, t_2, t_3,$ and t_4 in Eq. 27 by $n, n+1, n+k,$ and $n+k+1$ respectively, and dividing by σ^2 :

$$\rho_k = 1/2[(k+1)^{2H} - 2k^{2H} + (k-1)^{2H}].$$

The increment sequence is called fractional Gaussian noise. The auto-correlation in Eq. 29 exhibits long-range dependence, since $\rho_k \sim k^{2H-2}$ as $k \rightarrow \infty$ (follows by Taylor expansion). The use of fractional Brownian motion to model traffic is presented in [33]. The analytical solution for the distribution of the buffer occupancy is difficult [33]. Therefore, an approximation for the tail behavior is obtained. Results show that for large H , increasing the utilization requires a significant amount of storage space. The probability of cell loss decreases algebraically with buffer size and not exponentially as Markovian and ARMA models do. The Hurst parameter, H , can be estimated using the variance-time-plot with $H = 1 - \alpha/2$, where α is the slope of the plot. For generating fBm processes see [24, 34].

SUPERPOSITION OF HIGH VARIABILITY ON-OFF SOURCES

The traditional ON-OFF source models assume finite variance distributions for the sojourn time in ON and OFF periods. As a result, the aggregation of large number of such sources will not have significant correlation, except possibly in the short range [35].

An extension to such traditional ON-OFF models was first introduced by [36, 37] (as cited in [35]) by allowing the ON and OFF periods to have infinite variance (*high variability or Noah Effect*). The superposition of many such sources produces aggregate traffic that exhibits long-range dependence (also called the *Joseph Effect* [35, 38]).

The source model used in [38] can be described as follows:

- Denote $y_t^{(i)}$ the cell generation rate for source i at time t .
- Source i will transmit cells with rate R if it is in the ON period and will not transmit while in the OFF period.
- The time spent in the ON periods is an independent identically distributed random variables, denoted τ^i , and the distribution is a Pareto-type with finite mean a_τ and infinite variance, i.e.,

$$Pr\{\tau > t\} \sim t^{-\beta}, t \rightarrow \infty, 1 < \beta < 2. \quad (30)$$

- The OFF periods are identically distributed random variables with a generic distribution $\theta^{(i)}$ with finite mean a_θ .
- Let Y_t the total cell rate generated by M independent ON-OFF sources be:

$$Y_t = \sum_{i=1}^M y_t^i$$

$$E\{Y_t\} = MR \frac{a_\tau}{a_\tau + a_\theta}.$$

To avoid an infinite traffic intensity when $M \rightarrow \infty$, a_θ is increased in such a way that $\lambda = M/(a_\tau + a_\theta)$ is constant. Hence, in the limit as $M \rightarrow \infty$, $E\{Y_t\} = R\lambda a_\tau$.

It can be shown [38] that the aggregate process is long-range dependent and asymptotically self-similar with Hurst parameter $H = (3 - \beta)/2 > 0.5$, the auto-correlation $\rho_k \sim k^{1-\beta}$ for large k , and the limit as $m \rightarrow \infty$, $\rho_k^{(m)} \sim 1/2[(k+1)^{3-\beta} - 2k^{3-\beta} + (k-1)^{3-\beta}]$.

Analytical results for the queue length distribution of number of sources in the queue is obtained using M/G/1

queuing model. The probability of cell loss for large buffer sizes is given by (No proof was presented):

$$P_L = \frac{c}{\beta(\beta+1)} \lambda^\beta (Ra_\tau)^{1+\beta} L^{1-\beta}, \quad (31)$$

where L is the buffer size. Notice that the loss probability decreases with L algebraically and not exponentially as traditional Markovian traffic models do.

In [35], long-range dependent traffic (fractional Gaussian noise) with $H = (3 - \beta)/2$ is obtained by the aggregate of a large number of ON-OFF sources in which the ON and OFF periods have a Pareto type distribution with infinite variance. The analysis of two sets of high time-resolution traffic measurements from two Ethernet LAN's shows that the data at the source level have high variability (*Noah Effect*).

CONCLUSIONS

Traffic models are used in traffic engineering to predict network performance and to evaluate congestion control schemes. Traffic models vary in their ability to model various correlation structures and marginal distributions. Models that do not capture the statistical characteristics of the actual traffic result in poor network performance because they either over estimate, or under estimate the network performance. Traffic models must have a manageable number of parameters and the estimation of these parameters needs to be simple. Traffic models which are not analytically tractable can only be used to generate traffic traces. These traffic traces can be used in simulations.

Traffic models can be stationary or nonstationary. Stationary traffic models can be classified into two classes: short-range and long-range dependent. Short-range dependent models include traditional traffic models such as Markov processes and regression models. These traffic models are discussed in the second and third sections. The second section described Markov chains, semi-Markov chains, and Markov modulated processes. The third section described AR, ARMA, ARIMA, TES, and DAR regression models. Traditional traffic models are characterized by an auto-correlation structure that decays exponentially so that $\sum_k \rho_k < \infty$. This results in the variance of the sample mean, v_m , to decay as m^{-1} for large m , or equivalently, they tend to white noise for large m .

Long-range dependent traffic models, such as fractional ARIMA and fractional Brownian motion, are characterized by an auto-correlation structure that decays at a slower rate such that $\sum_k \rho_k \rightarrow \infty$. This results in the variance of the sample mean, v_m , to decay at a slower rate than m^{-1} even for large m .

Markovian and regression traffic models are short-range dependent traffic models. The queuing performance of the Markovian models is analytically tractable, while, in general, that of regression models is not. The computational complexity of the analytical solution of Markovian models increases as the number of states in the model increases. Since a small number of states is used to model voice sources, Markovian models are widely used in telephony. On the other hand, it is non-trivial to capture arbitrary probability distribution in Markovian models. Moreover, they can not be used to model traffic that exhibits long-range dependence.

Regression models are simple to generate. Therefore, they are used in simulations. Queuing of regression models is usually intractable. Therefore, regression models are often approximated by Markovian models in order to get approximate analytical solution. Regression models define the next random variable in the sequence by an explicit function of previous random variables. Hence, they are used to model sequences that do not vary much between successive observations, e.g.,

number of bits/frame of teleconferencing VBR video. AR, ARMA, DAR, and TES regression processes can only model stationary processes, while ARIMA regression process can model both stationary and some non-stationary processes.

In general, AR, ARMA, and ARIMA processes use Gaussian white noise because the sum of Gaussian random variables is a Gaussian. Therefore, in order to model an arbitrary distribution, a two-step transformation is needed to transform the resulting process from the Gaussian to the desired distribution. This transformation does not guarantee that the transformed process will have the same correlation structure as the original one.

DAR(p) and TES models have arbitrary distributions. DAR models have auto-correlation structures similar to that of AR(p) processes. They also enjoy analytical tractability by using their equivalent Markov chain models. TES models are non-linear regression models that use modulo-1 arithmetic. They can generate processes with different correlation structures with uniform probability distributions. TES models use a heuristic search to find the best TES process that can capture both auto-correlation structure and distribution of the empirical data. Recently, an automated solution was presented [39].

Examples of long-range dependent traffic models are given in (the fourth section). These include fractional Brownian motion, aggregate of ON-OFF high variability sources, and F-ARIMA. Fractional Brownian motion has only one parameter controlling the auto-correlation function. Therefore, there is no flexibility in modeling short-range dependence. The aggregation of large numbers of ON-OFF sources with infinite variance for the ON and OFF periods exhibits long-range dependence, and can be used to capture the asymptotic behavior of long-range dependent traffic. However, it is not clear how it will model the short-range behavior. F-ARIMA models have three parameters p , d , and q that control the auto-correlation structure. Therefore, they can capture both short-range and long-range dependence. The parameter d determines the long term behavior, ($H = d + 1/2$), whereas p and q allow for more flexibility in modeling the short-range properties [25]. Fractional Brownian motion (fractional Gaussian noise) and the Gaussian F-ARIMA have a Gaussian distribution and cannot match arbitrary empirical distributions. Hence, inversion methods need to be used. These methods, in general, affect the correlation structure of the original process.

It appears that a model that can capture short-range dependence, long-range dependence, and an arbitrary distribution is needed. A systematic and simple method that can decouple the estimation of long-range and short-range parameters in the model needs to be developed.

Finally, analytical performance solutions for nontraditional traffic models need to be investigated for a single node, as well as for an end-to-end network model.

ACKNOWLEDGMENT

Special thanks to Amarnath Mukherjee for his ideas, supervision, and fruitful discussions throughout the development of this work.

REFERENCES

[1] V. Frost and B. Melamed, "Traffic Modeling for Telecommunications Networks," *IEEE Commun. Mag.*, Mar. 1994.
 [2] D. Lucantoni, M. Neuts, and A. Reibman, "Methods for Performance Evaluation of VBR Video Traffic Models," *IEEE/ACM Trans. Networking*, vol. 2, Apr. 1994, pp. 176-80.
 [3] L. Kleinrock, *Queueing Systems*, vol. 1, John Wiley and Sons, 1975.
 [4] H. Heffes and D. Lucantoni, "A Markov Modulated Characterization of Packetized Voice and Data Traffic and Related Statistical Multiplexer Performance," *IEEE JSAC*, Sept. 1986, pp. 856-68.
 [5] I. Nikolaidis and I. Akyildiz, "Source Characterization and Statistical Multiplexing in ATM Networks," Tech. Rep. GIT-CC 92-24, Georgia Tech., 1992.

[6] J. Hui, *Switching and Traffic Theory for Integrated Broadband Networks*, Kluwer Academic, 1990.
 [7] B. Maglaris et al., "Performance Models of Statistical Multiplexing in Packet Video Communications," *IEEE Trans. Commun.*, vol. 36, July 1988.
 [8] P. Sen et al., "Models for Packet Switching of Variable-Bit-Rate Video Sources," *IEEE JSAC*, vol. 7, no. 5, 1989.
 [9] A. Papoulis, *Probability, Random Variables, and Stochastic Processes*, 3rd ed., McGraw Hill, 1991.
 [10] G. Box, G. Jenkins, and G. Reinsel, *Time Series Analysis*, 3rd ed., Prentice Hall, 1994.
 [11] C. Shim et al., "Modeling and Call Admission Control Algorithm of Variable Bit Rate Video in ATM Networks," *IEEE JSAC*, vol. 12, Feb. 1994.
 [12] D. Cohen and D. Heyman, "Performance Modeling of Video Teleconferencing in ATM Networks," *IEEE Trans. Circuits and Sys. for Video Tech.*, vol. 3, Dec. 1993, pp. 408-20.
 [13] D. Heyman et al., "Modeling Teleconference Traffic from VBR Video Coders," *Proc. ICC*, IEEE, 1994, pp. 1744-48.
 [14] D. Heyman, A. Tabatabai, and T. Lakshman, "Statistical Analysis and Simulation Study of Video Teleconference Traffic in ATM Networks," *IEEE Trans. Circuits and Sys. for Video Tech.*, vol. 2, Mar. 1992, pp. 49-59.
 [15] M. Hayes, *Statistical Digital Signal Processing and Modeling*, John Wiley, 1996.
 [16] R. Grunenfelder et al., "Characterization of Video Codecs as Autoregressive Moving Average Processes and Related Queuing System Performance," *IEEE JSAC*, vol. 9, Apr. 1991, pp. 284-93.
 [17] D. R. Cox, "Long-Range Dependence: A Review," *Statistics: An Appraisal*, 1984, Iowa State Univ. Press, pp. 55-74.
 [18] D. Jagerman and B. Melamed, "The Transition and Autocorrelation Structure of TES Processes," *Commun. Stat.-Stochastic Models*, 1992.
 [19] B. Melamed, "TES: A Class of Methods for Generating Autocorrelated Uniform Variates," *ORSA J. Comp.*, vol. 3, no. 4, pp. 317-29, 1991.
 [20] W. Leland et al., "On the Self-Similar Nature of Ethernet Traffic (Extended Version)," *IEEE/ACM Trans. Networking*, Feb. 1994, pp. 1-15.
 [21] S. Klivanski, A. Mukherjee, and C. Song, "On Long-Range Dependence in NSFNET Traffic," Tech. Rep. GIT-CC-94-61, Georgia Tech., 1994.
 [22] B. B. Mandelbrot and J. R. Wallis, "Some Long-Run Properties of Geophysical Records," *Water Resources Res.*, vol. 5, 1969, pp. 321-40.
 [23] J. Hosking, "Modeling Persistence in Hydrological Time Series Using Fractional Differencing," *Water Resources Res.*, vol. 20, Dec. 1984, pp. 1898-1908.
 [24] B. Mandelbrot and J. Wallis, "Computer Experiments with Fractional Gaussian Noises," *Water Resources Res.*, vol. 5, Feb. 1969, pp. 228-67.
 [25] J. Beran, *Statistics for Long-Memory Processes*, Chapman and Hall, 1994.
 [26] J. Beran et al., "Long-Range Dependence in Variable-Bit-Rate Video Traffic," *IEEE Trans. Commun.*, 1995, pp. 1566-79.
 [27] W. Willinger, "When Traffic Measurements Defy Traditional Traffic Models (and Vice Versa): Traffic Modeling for High-Speed Networks," Presentation at Georgia Tech, 1994.
 [28] G. Samorodnitsky and M. Taqqu, *Stable Non-Gaussian Random Processes*, Chapman and Hall, 1994.
 [29] J. Hosking, "Fractional Differencing," *Biometrika*, 1981, pp. 165-76.
 [30] C. H. and M. Devetsikiotis, I. Lambadaris, and A. Kaye, "Self-Similar Modeling of Variable Bit Rate Compressed Video: A Unified Approach," *Proc. ACM SIGCOM '95*, 1995.
 [31] A. Adas and A. Mukherjee, "On Resource Management and QoS Guarantees for Long Range Dependent Traffic," *Proc. IEEE INFOCOM '95*, 1995.
 [32] S. Karlin and H. Taylor, *A First Course in Stochastic Processes*, Academic, 2 ed., 1975.
 [33] I. Norros, "On the Use of Fractional Brownian Motion in the Theory of Connectionless Traffic," *IEEE JSAC*, Aug. 1995, pp. 953-62.
 [34] S. Kogon and D. Manolakis, "Efficient Generation of Long-Memory Signals Using Lattice Structure," preprint, 1995.
 [35] W. Willinger et al., "Self-Similarity through High Variability: Statistical Analysis of Ethernet LAN Traffic at the Source Level," *Proc. ACM SIGCOMM '95*, 1995, pp. 100-13.
 [36] B. Mandelbrot, "Long-Run Linearity, Locally Gaussian Processes, H-Spectrum and Infinite Variance," *Int'l. Economic Rev.*, vol. 10, 1969, pp. 82-113.
 [37] M. Taqqu and J. Levy, "Using Renewal Processes to Generate Long-Range Dependence and High Variability," *Dependence in Probability and Statistics*, Boston, MA, 1986, pp. 73-89.
 [38] N. Likhanov, B. Tsybakov, and N. Georganas, "Analysis of an ATM Buffer with Self-Similar (Fractal) Input Traffic," *Proc. IEEE INFOCOM '95*, Apr. 1995.
 [39] B. Melamed and P. Jelenkovic, "Automated TES Modeling of Compressed Video," *Proc. IEEE INFOCOM '95*, 1995, pp. 746-52.

BIOGRAPHY

ABDELNASER ADAS received a B.Sc. in electrical engineering from University of Jordan in 1988, an M.Sc. in electrical engineering from New Jersey Institute of Technology in 1993, and a Ph.D. from the Georgia Institute of Technology Electrical and Computer Engineering Department. Research interests are in network resource management, statistical performance analysis, traffic modeling, multimedia applications, and network services to the home.